Letter

Estimation of global level density parameters using an unscented transform Kalman filter technique

Mahesh Choudhary,* Aman Sharma,† Namrata Singh, Punit Dubey, Mahima Upadhyay, Sriya Paul, Shweta Singh, Utkarsha Mishra, and A. Kumar‡
Department of Physics, Banaras Hindu University, Varanasi-221005, India

S. Dasgupta and J. Datta
Analytical Chemistry Division, Bhabha Atomic Research Centre, Variable Energy Cyclotron Centre, Kolkata-700064, India

(Received 31 January 2024; revised 13 March 2024; accepted 20 March 2024; published 11 April 2024)

This study focuses on estimating the level density parameters for niobium (Nb) using the unscented transform Kalman filter technique. Niobium is widely utilized in accelerator components, particularly in superconducting radiofrequency cavities. To better understand the design of accelerator components and experimental setups, accurate information on both theoretical predictions and experimental results, including the uncertainties of nuclear reactions involving niobium, is essential. In this study, we have used the unscented transform Kalman filter technique to estimate level density parameters and their correlation matrix for ^{93}Nb$(\alpha, 2n)^{95}$Tc and ^{93}Nb$(\alpha, n)^{96}$Tc reactions through the TALYS nuclear code. We have used the measured experimental nuclear reaction cross sections from this study to estimate the level density parameters for the above nuclear reactions. A comprehensive analysis of uncertainty propagation has been also conducted, encompassing both theoretical predictions and experimentally measured nuclear reaction cross sections. We have calculated uncertainties in both the theoretical calculations using the Monte Carlo method and experimentally measured reaction cross sections through covariance analysis for these nuclear reactions. We have also calculated the correlation matrix of the experimentally measured cross sections for the ^{93}Nb$(\alpha, n)^{95}$Tc and ^{93}Nb$(\alpha, n)^{96}$Tc nuclear reactions.

DOI: 10.1103/PhysRevC.109.L041603

Advancing nuclear technologies is closely linked with the availability of high quality data on nuclear reactions. Particularly, comprehensive data on α projectiles interacting with different target materials across a broad spectrum of projectile energies is important for the evolution of future nuclear technologies. Nowadays in nuclear science, most attention is focused on the estimation of nuclear data uncertainties and their correlations [1,2]. This information plays an important role in calculating and understanding the uncertainties inherent in the design parameters of nuclear facilities. There are many theoretical models used in which we can make predictions of nuclear reactions. These models are characterized by a set of parameters, which are typically estimated by comparing model predictions with available experimental data. The accuracy and reliability of these parameters fundamentally influence the outcomes of the models. Therefore, the understanding of uncertainties and correlations inherent in these model parameters is very important. Niobium is often used in the construction of superconducting radiofrequency (SRF) cavities for accelerators [3–5]. Estimating the level density parameters helps in predicting the nuclear reaction of niobium under various conditions, facilitating the design and testing of accelerator components.

In the present work, we have estimated the level density model parameters and their correlation for the ^{93}Nb$(\alpha, 2n)^{95}$Tc and ^{93}Nb$(\alpha, n)^{96}$Tc nuclear reaction utilizing the unscented transform Kalman filter technique through TALYS nuclear code. Level density represents a crucial ingredient in statistical model calculations of nuclear reaction cross sections, playing a pivotal role in various applications. These applications range from astrophysical calculations, where level density is used in determining thermonuclear rates for nucleosynthesis, to the design of fission or fusion reactors. Their significance becomes important in the statistical models employed for predicting nuclear reactions, particularly at excitation energies where discrete level information is either absent or incomplete. In combination with the optical model potential, a suitable level density model is important for theoretical analysis of nuclear reactions. In this study, we have used measured experimental nuclear reaction cross sections to optimize the level density parameters for ^{93}Nb$(\alpha, 2n)^{95}$Tc and ^{93}Nb$(\alpha, n)^{96}$Tc nuclear reactions. To obtain experimental cross sections of these nuclear reactions, we have used the stacked foil activation technique [6–9]. To calculate the uncertainty associated with the theoretical predictions of the ^{93}Nb$(\alpha, 2n)^{95}$Tc and ^{93}Nb$(\alpha, n)^{96}$Tc nuclear reactions, we employed the Monte Carlo method. This involved utilizing updated parameters from this study and their associated uncertainties. The incorporation of these uncertainties provides a comprehensive understanding of the reliability and vari-

*maheshchoudhary921@gmail.com
†Present address: Nuclear and Chemical Science Division, Lawrence Livermore National Laboratory, Livermore, CA 94551, USA.
‡Corresponding author: ajaytyagi@bhu.ac.in

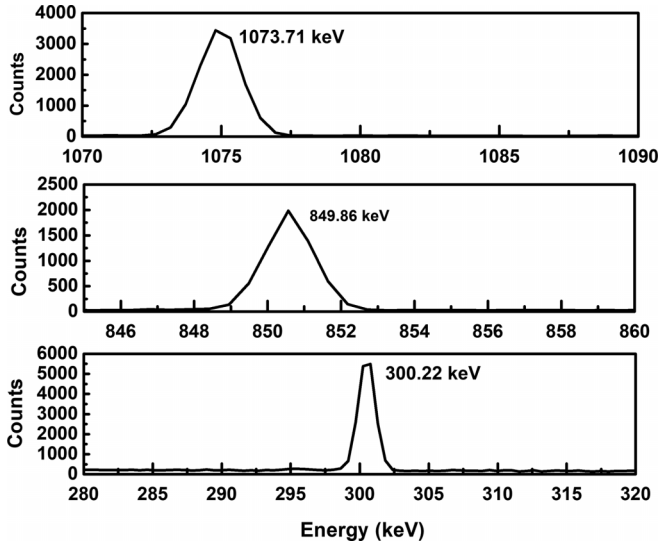

FIG. 1. The γ-ray spectrum of the irradiated target and monitor foil.

ability inherent in the theoretical prediction of these nuclear reactions. In addition to the theoretical uncertainty analysis, we have calculated the correlation matrix of the measured cross sections for the ^{93}Nb$(\alpha, 2n)^{95}$Tc and ^{93}Nb$(\alpha, n)^{96}$Tc nuclear reactions. The correlation matrix offers insights into the inter-dependencies between measured reaction cross sections, enriching our understanding of the experimental data. Furthermore, the uncertainty in the measured reaction cross sections has been systematically calculated through covariance analysis.

The experiment was performed at the Variable Energy Cyclotron Centre (VECC), Kolkata, India, utilizing the K-130 cyclotron. We employed the stacked foil activation technique and performed off-line γ-ray spectroscopy using the HPGe detector. The ^{93}Nb foil is used as a target material likewise, we included ^{nat}Al and ^{nat}Cu foils in the stacks, serving as energy degraders and monitors, respectively. To ascertain the energy degradation in each foil, we used the stopping and range of ions in matter (SRIM) code [10,11]. The thicknesses of the Nb, Al, and Cu foils were 10.6 mg/cm^2, 6.7 mg/cm^2, and 9.9 mg/cm^2, respectively. We constructed the stacked targets using three sets of Cu-Nb-Al foils and two sets of Cu-Nb-Al foils, each measuring 10×10 mm^2. For beam monitoring and validation of incident beam intensity and energy, we placed a ^{nat}Cu foil before each Nb foil. The comprehensive methodology for efficiency calibration of the high purity germanium (HPGe) detector and the computation of experimental nuclear reaction cross sections have been outlined in our prior publications [12,13]. Figure 1 displays the γ-ray spectrum corresponding to the irradiated target and monitor foils.

The level density plays a crucial role in determining nuclear reaction cross sections. It describes the distribution of nuclear energy levels concerning excitation energy, influencing the presence of excited states in compound nuclei and, consequently, impacting the reaction cross section. The total Fermi gas level density at energy E_x is given by the following equation [14]:

$$\rho_F^{\text{tot}}(E_x) = \frac{1}{\sqrt{2\pi\sigma}} \frac{\sqrt{\pi}}{12} \frac{\exp(2\sqrt{aU})}{a^{1/4}U^{5/4}}, \tag{1}$$

where

$$U = E_x - \Delta. \tag{2}$$

Here, Δ is the energy shift parameter and it is often chosen or adjusted to reproduce the experimentally observed odd-even effects in nuclear masses. The energy shift is defined as $\Delta = \chi \frac{12}{\sqrt{A}} + \delta$, where χ have value -1 for odd-odd, 1 for even-even, 0 for odd-even nuclei, and δ an adjustable parameter to fit experimental data. In Eq. (1), a and σ are the level density parameter and the spin cut-off parameter, respectively. The level density parameter (a) is defined as

$$a(E_x) = \tilde{a}\left(1 + \delta W \frac{1 - \exp(-\gamma U)}{U}\right), \tag{3}$$

where $\tilde{a}$ represents the asymptotic level density value given as

$$\tilde{a} = \alpha A + \beta A^{2/3}. \tag{4}$$

In the above equation, A represents the mass number. The damping parameter (γ) in this context is determined systematically using the following formula:

$$\gamma = \frac{\gamma_1}{A^{1/3}}. \tag{5}$$

From Eqs. (1) to (5) $\sigma, \alpha, \beta, \delta, \gamma_1$ are adjustable global parameters that can be calculated by comparing the theoretical model prediction with experimental data.

The unscented transform Kalman filter (UTKF) stands as a tool for parameter and state estimation. In the given context, to outline the parameter estimation process for the present problem, consider an N-dimensional vector representing the experimental measurements (denoted as d) and a prior estimate of the parameter vector (θ_0) of dimension L with its covariance matrix P_0. Let $G(\theta_k)$ represent the model to which experimental results are compared, with the index k denoting calculations for the kth experimental data set ($k = 1, 2, 3,..., \infty$). The time update equations for estimating parameters for the kth experimental data set are expressed as $\theta_k^- = \theta_{k-1}$ and $P_{\theta k}^- = P_{k-1} + R_{k-1}^r$. Here, R_{k-1}^r signifies the process noise covariance. Utilizing the unscented transform, we can generate an $L \times (2L + 1)$ dimensional matrix (W) containing $(2L + 1)$ sets of σ points, as outlined below [15]:

$$W_{k|k-1} = \left[\theta_k^- \quad \theta_k^- + \sqrt{(L+\lambda)P_{\theta_k}^-} \quad \theta_k^- - \sqrt{(L+\lambda)P_{\theta_k}^-}\right]. \tag{6}$$

The associated weights for the σ points are defined by the following expressions, with superscripts (m) and (c) denoting their application in calculating the mean and covariances, respectively:

$$w_0^{(m)} = \frac{\lambda}{L+\lambda}, \tag{7}$$

$$w_0^{(c)} = \frac{\lambda}{L+\lambda} + (1 - \alpha^2 + \beta), \tag{8}$$

$$w_i^{(m)} = w_i^{(c)} = \frac{1}{2(L+\lambda)} \quad \text{for } i = 1, 2, \ldots, 2L. \tag{9}$$

Here, $\lambda = \alpha^2(L+\kappa) - L$ and α, κ, β are the scaling parameters used for approximating the probability distribution function of the input parameters. Utilizing $(2L+1)$ sets of parameters, we can construct an $N \times (2L+1)$ dimensional matrix (D) encompassing $(2L+1)$ sets of model predictions generated by the model function $G(\theta_k)$. From this ensemble, we perform calculations to determine the quantities required to update the parameters and their associated covariance matrices. This involves the following equations:

$$\theta_k = \theta_k^- + K_k(d_k - \hat{d}_k), \tag{10}$$

$$P_{\theta_k} = P_{\theta_k}^- - K_k P_{\hat{d}_k \hat{d}_k} K_k^T. \tag{11}$$

Here, K_k denotes the Kalman gain. Subsequently, for the next set of experimental measurements, i.e., for the $(k+1)$th set, these updated parameters and their covariance matrix are regarded as a prior estimation. Covariance analysis is a tool that helps us deal with uncertainties and connections between different measurements. In fields like nuclear science, where we are working with a number for reactors and nuclear medicine, a detailed description of experimental uncertainties with a comprehensive correlation matrix is important. The covariance matrix for the measured cross sections symbolized as I_σ, can be represented as the result of multiplying certain matrices, as given by [16,17]

$$I_\sigma = F_y C_y F_y^T, \tag{12}$$

where

$$F_{y_{ij}} = \frac{\partial \sigma_i}{\partial y_j}; \quad (i = 1, 2, \ldots, m;\ j = 1, 2, \ldots,\ n), \tag{13}$$

$$C_y(y_j, y_k) = Cor(y_j, y_k) \cdot (\Delta y_j \cdot \Delta y_k). \tag{14}$$

In Eqs. (12), (13), and (14), the symbol C_y represents the covariance matrix (C_y) of various attributes such as counts of the γ rays in the target and monitor foils, the intensity of γ rays, the decay constant of produced radionuclide, efficiency of HPGe detector, number of particles in the target and monitor foils, etc. Additionally, the matrix F_y is employed to denote the sensitivity matrix. The uncertainties associated with the various parameters contributing to the measured nuclear reaction cross sections are provided in Table I.

On the other hand, we employed the Monte Carlo method [18] to calculate uncertainties in the theoretical prediction for both ^{93}Nb$(\alpha, 2n)\,^{95}$Tc and ^{93}Nb$(\alpha, n)\,^{96}$Tc nuclear reactions. This method aims to analyze how uncertainties in nuclear input parameters influence the reaction cross section. By exploring a range of parameter values within their respective uncertainty bounds, we can generate a distribution of cross sections. This distribution provides valuable insights into the variability of results arising from uncertainties in the theoretical model. The Monte Carlo method involves randomly sampling input model parameters from their joint probability distribution function. Subsequently, these randomly selected parameter sets were used to conduct simulations of the theoretical model using the TALYS nuclear code. We conducted 100 random samplings of the updated parameters which are given in Table II, exploring values within the specified ranges of uncertainties. Furthermore, we calculated the 95% confidence interval for theoretical cross section uncertainties within the incident α energy range of 20 to 48 MeV. This interval provides a region where the theoretical cross section is anticipated to fall with a confidence level of 95%. This range serves as an assessment of the precision and accuracy of the theoretical predictions, accounting for the collective impact of all input parameter uncertainties. The nuclear reaction cross sections for ^{93}Nb$(\alpha, 2n)\,^{95}$Tc and ^{93}Nb$(\alpha, n)\,^{96}$Tc reactions, computed using both the initial and a new set of parameters, are presented in Figs. 3 and 4, respectively. These figures are presented along with the measured experimental data obtained from this study and taken from the EXFOR database [19]. We determined a set of five-level density parameters and one optical model parameter (a_v), detailed in Table II. To initiate our estimations, we employed the Back-shifted Fermi gas model (BFM) [20], and the uncertainties of the initial parameters were used from Ref. [21]. Employing the unscented transform method, we have generated 13 sets of σ points $(2 \times 6 + 1 = 13)$. We estimated the parameters using experimentally measured results from this study of the ^{93}Nb$(\alpha, 2n)\,^{95}$Tc nuclear reaction. Remarkably, there was no need to readjust the level density parameters for the ^{93}Nb$(\alpha, n)\,^{96}$Tc reaction. Instead, we employed updated parameters obtained by fitting the ^{93}Nb$(\alpha, 2n)\,^{95}$Tc nuclear reaction cross section for theoretical

TABLE I. The uncertainties in the various parameters contributing to the uncertainty in the measured reaction cross sections.

Parameters x_i	^{93}Nb$(\alpha, 2n)\,^{95}$Tc Δx_i (%)	^{93}Nb$(\alpha, n)\,^{96}$Tc Δx_i (%)
σ_m	4–5	4–5
C_m	0.5–2	0.5–2
C_s	1–7	0.5–3
λ_s	0.50	1.64
λ_m	0.02	0.02
I_s	1.07	4.08
I_m	0.72	0.72
N_s	1.6	1.6
N_m	1.7	1.7
ϵ_s	2.41	3.09
ϵ_m	1.77	1.77

TABLE II. Comparison of the initial and updated sets of parameters, along with the associated percentage uncertainties given in parentheses, as explored in this study.

(S.No)	Parameters	Initial	Updated
1	σ	1 (30)	1.65 (13.19)
2	α	0.0722 (30)	0.0889 (20.65)
3	β	0.1952 (30)	0.1951 (25.28)
4	δ	0.1730 (30)	0.1730 (30)
5	γ	0.4102 (30)	0.3976 (30.73)
6	a_V	1 (5)	1.1543 (4.90)

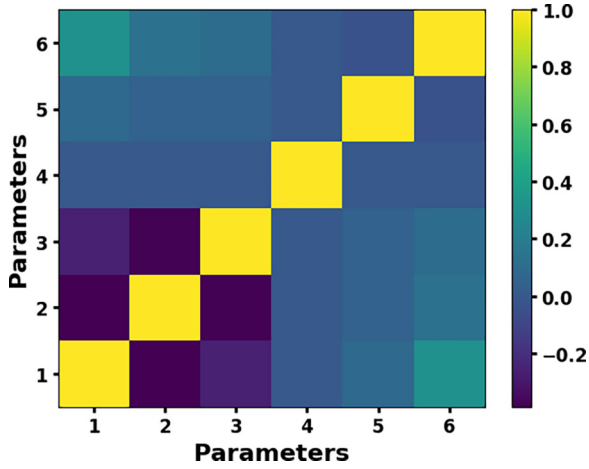

FIG. 2. The parameter correlation matrix, where parameters are organized based on their serial numbers as defined in Table II.

calculations of the ^{93}Nb(α, n) ^{96}Tc nuclear reaction. Figure 2 illustrates the correlation matrix of the newly obtained set of parameters. Figures 3 and 4 show that the updated set of level density parameters provides a more accurate visual match to the experimental data compared to the initial parameter set. Table II shows both the updated and initial parameters with their uncertainties and Fig. 2 illustrates the correlation matrix of the updated parameter (arranged based on their serial numbers, as defined in Table II). We have specifically compared the asymptotic value ($\tilde{a}$) of level density parameter (a) obtained from our present study with the values reported in Von Egidy's work [22]. The asymptotic value ($\tilde{a}$) of level density parameter (a) is calculated by utilizing the updated global level density parameters from our study, whereas Von Egidy's values were derived from Table III of Ref. [22]. The comparative results for the asymptotic value ($\tilde{a}$) of level density parameters (a) are shown in Table III.

The comparison of measured experimental cross section data with existing experimental data from EXFOR for the ^{93}Nb$(\alpha, 2n)$ ^{95}Tc nuclear reaction, as shown in Fig. 3. The figure also includes the 95% confidence interval for

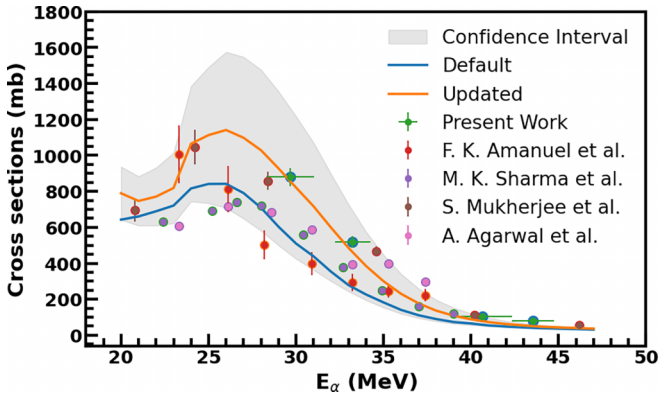

FIG. 3. Comparison of the experimentally measured cross section for ^{93}Nb$(\alpha, 2n)$ ^{95}Tc with the existing experimental data from EXFOR as well as confidence interval of theoretical prediction.

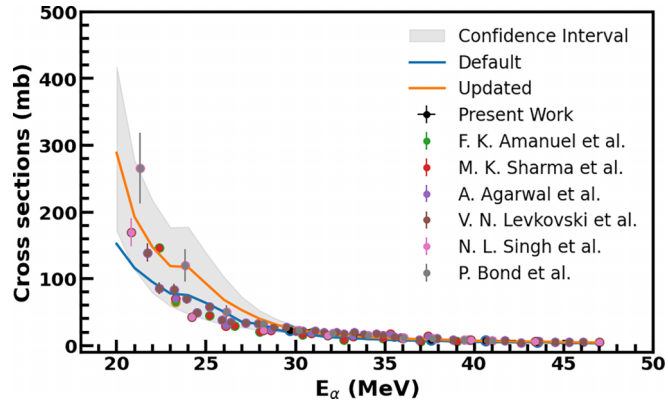

FIG. 4. Comparison of the experimentally measured cross section for ^{93}Nb(α, n) ^{96}Tc with the existing experimental data from EXFOR as well as confidence interval of theoretical prediction.

theoretical cross-section uncertainties within the incident α energy range of 20 to 48 MeV for this reaction. The resulting radionuclide, ^{95}Tc, produced from ^{93}Nb$(\alpha, 2n)$ nuclear reaction has a half-life of 20 h. The reaction cross sections for the ^{93}Nb$(\alpha, 2n)$ ^{95}Tc nuclear reaction were calculated using a γ ray with an energy of 1073.71 keV and an intensity of $I_\gamma = 3.74\%$. In Table IV, we presented the measured reaction cross sections within the incident α energy range of about 28 to 45 MeV, along with their uncertainties and the covariance matrix for the ^{93}Nb$(\alpha, 2n)$ ^{95}Tc nuclear reaction. From Fig. 3, the measured experimental reaction cross section and the data from Mukherjee *et al.* [23] are in good agreement. Additionally, it is also observed from Fig. 3 that all experimental results from Mukherjee *et al.*, Amanuel *et al.*, Sharma *et al.*, and Agarwal *et al.* [23–26] fall within the 95% confidence interval of the theoretical predictions for the ^{93}Nb$(\alpha, 2n)$ ^{95}Tc nuclear reaction.

The measured experimental cross section data with existing experimental data from EXFOR for the ^{93}Nb(α, n) ^{96}Tc nuclear reaction, is shown in Fig. 4. The figure also includes the 95% confidence interval for theoretical cross-section uncertainties within the incident α energy range of 20 to 48 MeV for this reaction. The resulting radionuclide, ^{96}Tc, produced from ^{93}Nb(α, n) nuclear reaction has a half-life of 4.28 d. The reaction cross sections for the ^{93}Nb(α, n) ^{96}Tc nuclear reaction were calculated using a γ ray with an energy of 849.86 keV and an intensity of $I_\gamma = 98\%$. In Table V, we present the measured reaction cross sections within the incident α energy range of 28 to 45 MeV, along with their uncertainties and the correlation matrix for the ^{93}Nb(α, n) ^{96}Tc nuclear reaction. The measured experimental reaction cross-section and

TABLE III. The comparative results for asymptotic value ($\tilde{a}$) of level density parameter (a).

Nuclei	From present work [Asymptotic value ($\tilde{a}$)]	From Von Egidy [22] [Asymptotic value ($\tilde{a}$)]
^{95}Tc	12.51	11.25
^{96}Tc	12.74	11.36

TABLE IV. The obtained reaction cross section with correlation matrix and their uncertainty for ^{93}Nb$(\alpha, 2n)^{95}$Tc at different incident α energies.

E_α (MeV)	Cross section (mb) ($\sigma \pm \bigwedge \sigma$)	Correlation matrix			
29.67 ± 1.38	880.63 ± 50.02	1			
33.23 ± 1.0	518.26 ± 31.16	0.373	1		
40.54 ± 1.69	102.43 ± 8.09	0.299	0.283	1	
43.53 ± 1.20	78.13 ± 7.35	0.252	0.238	0.194	1

the data from Amanuel *et al.*, Sharma *et al.*, Agarwal *et al.*, Levkovski *et al.*, Singh *et al.*, Bond *et al.* [24–29] are in good agreement. Additionally, it is also observed from Fig. 4 that all the experimental results fall within the 95% confidence interval of the theoretical predictions for the ^{93}Nb$(\alpha, n)^{96}$Tc nuclear reaction.

In this work, we have presented a comprehensive study on the uncertainty quantification of the ^{93}Nb$(\alpha, 2n)^{95}$Tc and ^{93}Nb$(\alpha, n)^{96}$Tc nuclear reaction. The experimentally measured nuclear reaction cross sections at different incident α energies have been observed to be correlated. The study found uncertainties in the measured reaction cross sections to be within 10% for both the nuclear reactions ^{93}Nb$(\alpha, 2n)^{95}$Tc and ^{93}Nb$(\alpha, n)^{96}$Tc. Additionally, the uncertainties in the theoretical predictions were found to be within 15%. From this study, we have concluded that there exists a correlation between the level density parameters and the optical model parameter a_v. The parameter σ demonstrates an anticorrelation with α and β, while exhibiting a correlation with γ and a_v. On the other hand, the δ parameter is found to be uncorrelated with all other parameters investigated in this study. Moreover, the optical model parameter a_v displays an anticorrelation with γ and is correlated with all other parameters under consideration. The experimental results from this study and available data from the EXFOR are in good agreement. From this study, we also found that all experimentally measured cross sections for the ^{93}Nb$(\alpha, 2n)^{95}$Tc and ^{93}Nb$(\alpha, n)^{96}$Tc nuclear reactions are consistent within the theoretical bands of uncertainties. Since niobium plays an integral role in the construction of superconducting radiofrequency (SRF) cavities for accelerators, this comparative study on niobium of experimental and theoretical aspects serves to enhance our understanding, directly influencing the design and performance of crucial SRF cavities in accelerator technologies.

The author (M.C.) acknowledges the Senior Research Fellowships provided by the Council of Scientific and Industrial Research (CSIR), Government of India, under File No. 09/013(882)/2019-EMR-1.

TABLE V. The obtained reaction cross section with correlation matrix and their uncertainty for ^{93}Nb$(\alpha, n)^{96}$Tc at different incident α energies.

E_α (MeV)	Cross section (mb) ($\sigma \pm \bigwedge \sigma$)	Correlation matrix				
29.67 ± 1.38	22.76 ± 1.51	1				
33.23 ± 1.0	15.14 ± 1.01	0.582	1			
37.59 ± 1.98	8.55 ± 0.60	0.550	0.548	1		
40.64 ± 1.69	7.16 ± 0.52	0.534	0.532	0.516	1	
43.53 ± 1.20	5.53 ± 0.41	0.516	0.514	0.499	0.484	1

[1] W. E. Ormand, Phys. Rev. C **56**, R1678(R) (1997).
[2] C. R. Weisbin, E. M. Oblow, J. H. Marable, R. W. Peelle, and J. L. Lucius, Nucl. Sci. Eng. **66**, 307 (1978).
[3] S. Casalbuoni, E. A. Knabbe, J. Kötzler, L. Lilje, L. von Sawilski, P. Schmüser, and B. Steffen, Nucl. Instrum. Methods Phys. Res. A **538**, 45 (2005).
[4] G. Ciovati, J. Appl. Phys. **96**, 1591 (2004).
[5] A. Grassellino, A. Romanenko, D. Sergatskov, O. Melnychuk, Y. Trenikhina, A. Crawford, A. Rowe, M. Wong, T. Khabiboulline, and F. Barkov, Supercond. Sci. Technol. **26**, 102001 (2013).
[6] M. S. Uddin, K. S. Kim, M. Nadeem, S. Sudár, and G. N. Kim, Eur. Phys. J. A **53**, 100 (2017).
[7] S. Takács, M. P. Takács, A. Hermanne, F. Tárkányi, and R. A. Rebeles, Nucl. Instrum. Methods Phys. Res. B **297**, 44 (2013).
[8] S. Takács, M. P. Takács, A. Hermanne, F. Tárkányi, and R. A. Rebeles, Nucl. Instrum. Methods Phys. Res. B **278**, 93 (2012).
[9] T. Siiskonen, J. Huikari, T. Haavisto, J. Bergman, S.-J. Heselius, J.-O. Lill, T. Lönnroth, and K. Peräjärvi, Appl. Radiat. Isot. **67**, 2037 (2009).
[10] J. F. Ziegler, J. P. Biersack, and M. D. Ziegler, SRIM-The Stopping and Range of Ions in Matter, SRIM Co., 2008 (2018), http://www.SRIM.org.
[11] P. Sigmund and A. Schinner, Nucl. Instrum. Methods Phys. Res. B **410**, 78 (2017).

[12] A. Gandhi, A. Sharma, R. Pachuau, B. Lalremruata, M. Mehta, P. N. Patil, S. V. Suryanarayana, L. S. Danu, B. K. Nayak, and A. Kumar, Eur. Phys. J. A **57**, 1 (2021).
[13] M. Choudhary, A. Sharma, N. Singh, A. Gandhi, S. Dasgupta, J. Datta, K. Katovsky, and A. Kumar, Nucl. Phys. A **1038**, 122720 (2023).
[14] A. J. Koning, S. Hilaire, and S. Goriely, Nucl. Phys. A **810**, 13 (2008).
[15] A. Sharma, A. Gandhi, and A. Kumar, Phys. Lett. B **815**, 136179 (2021).
[16] D. L. Smith and N. Otuka, Nucl. Data Sheets **113**, 3006 (2012).
[17] B. Lawriniang, R. Ghosh, S. Badwar, S. S. Yerraguntla, B. Jyrwa, H. Naik, Y. P. Naik, and S. V. Suryanarayana, J. Radioanal. Nucl. Chem. **319**, 695 (2019).
[18] A. Sharma, A. Gandhi, and A. Kumar, Phys. Rev. C **106**, L041601 (2022).
[19] IAEA-EXFOR Experimental Nuclear Reaction Database, https://www-nds.iaea.org/exfor, retrieved January 2024.
[20] W. Dilg, W. Schantl, H. Vonach, and M. Uhl, Nucl. Phys. A **217**, 269 (1973).
[21] A. J. Koning and D. Rochman, Nucl. Data Sheets **113**, 2841 (2012).
[22] T. von Egidy and D. Bucurescu, Phys. Rev. C **72**, 044311 (2005).
[23] S. Mukherjee, N. L. Singh, G. K. Kumar, and L. Chaturvedi, Phys. Rev. C **72**, 014609 (2005).
[24] F. K. Amanuel, B. Zelalem, A. K. Chaubey, A. Agarwal, and I. A. Rizvi, Chin. J. Phys. **49**, 884 (2011).
[25] M. K. Sharma, H. D. Bhardwaj, Unnati, P. P. Singh, B. P. Singh, and R. Prasad, Eur. Phys. J. A **31**, 43 (2007).
[26] A. Agarwal, I. A. Rizvi, and A. K. Chaubey, Phys. Rev. C **65**, 034605 (2002).
[27] V. N. Levkovski, Inter-Vesi, Moscow, USSR (1991).
[28] N. L. Singh, S. Agarwal, and J. R. Rao, J. Phys. Soc. Jpn. **59**, 3916 (1990).
[29] P. Bond and S. Jha, Phys. Rev. C **2**, 1887 (1970).